Dynamic analysis of holographic gratings in a multi-wavelength visible light sensitive photopolymer*

Chen Ke(陈 珂), Cheng Jian-Qun(成建群),
Wang Yan(王 艳), and Huang Ming-Ju(黄明举)†

Institute of Optics and Photoelectronic Technology, College of Physics and Electronics, Henan University, Kaifeng 475004, *China*

(Received 2 November 2008; revised manuscript received 15 April 2009)

A dynamic theoretical model of photochemistry and hologram formation in holographic photopolymer is established, and the dynamic development process of holographic gratings in the photopolymer is discussed with the model. A novel multi-wavelength visible light sensitive photopolymer for holographic storage is prepared. The influence of exposure wavelength on holographic storage characteristics is analysed. By fitting the experimental data of transmittance and diffraction efficiency to a function of time with different exposure intensities and wavelengths, the variations of dynamic parameters of photochemistry and photopolymerization diffusion are presented.

Keywords: photopolymer gratings, transmittance, diffraction efficiency, kinetics
PACC: 4240, 4270G, 8250

1. Introduction

Owing to the high density, mass capacity, high redundancy and fast data transfer rate, holographic data storage technology has become an important research field in optical information storage.[1] As superhuge capacity holographic storage materials, photopolymers have great advantages: low cost, high diffraction efficiency, wide dynamic range, high photosensitivity and dry real-time processing, thereby having aroused the extensive concern of the scientific community.[2] Most results of research have shown that the dynamic development process of holographic gratings in the photopolymer is connected with the photobleaching of dyes and the photopolymerization diffusion of monomers.[3−5] The photobleaching mechanism is mostly dependent on the absorption intensity of dyes and the rate of photochemical reaction,[6−8] and information on holographic gratings originates from the interaction between monomer polymerization and diffusion.[9−14] In the theoretical model of photopolymerization, some parameters are very important for holographic characteristics of photopolymer materials, such as the molar-absorption coefficient and quantum yield of dyes, the polymerization rate and diffusion time constant of monomers, the photobleaching rate, the photosensitivity and the refractive index modulation. They are usually estimated by fitting experimental data to the theoretical model.[9,10]

In holographic storage, the improvement of data recording density is dependent on diversified multiplexing methods such as wavelength multiplexing,[15] angular multiplexing[16] and phase multiplexing.[17] The polyvinyl alcohol (PVA)–acrylamide (AA) photopolymer studied in this paper is a multi-wavelength visible light sensitive holographic storage material, so it can satisfy the needs of many multiplexing methods.

It has been seldom reported that the whole dynamic processing of holographic gratings in the multi-wavelength visible light sensitive photopolymer is studied. In the present work, we take into account the influence of noise gratings at different wavelengths, and check the applicability of a modified dynamic diffraction efficiency model to a PVA–AA photopolymer. We also compare the theoretical and the experimental results about volume transmission–diffraction gratings recorded characteristics based on PVA–AA photopolymer with DuPont photopolymer. Combined with the photosensitive property of the photopolymer, dynamic characteristic parameters of material are retrieved by fitting experimental data for single and multiple wavelength irradiations to the macromolecule photochemical model, and their variations at different exposure wavelengths are studied. They are propitious to predicting new behaviours in high density data holographic storage such as the optimization

*Project supported by the Natural Science Foundation of Henan University, China (Grant No. 06ZDZR002).
†Corresponding author. E-mail: hmingju@163.com
© 2010 Chinese Physical Society and IOP Publishing Ltd

of the material for successive-wavelength-multiplexing recording and multi-wavelength storage.

2. Theoretical model

Figure 1 shows a schematic diagram of hologram formation in a photopolymer medium. The signal beam and the reference beam are used to generate an interference pattern inside the medium. In the bright areas, the initiators which are excited generate radicals. The monomers are polymerized by the radical polymerization reaction. Simultaneously, the monomer density in the bright areas decreases and non-polymerized monomers diffuse from the dark area to the bright area. With the advancement of a termination process, a difference in refractive index between the bright and dark areas is created by polymerization and monomer diffusion, so that the illumination beam profile can be recorded as the difference in refractive indices.

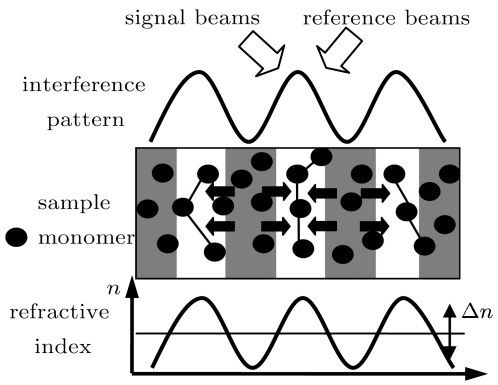


Fig. 1. Formation of holographic gratings.

2.1. Photochemical mechanism

When the photosensitive dye molecule is exposed to light of a suitable wavelength, it absorbs a photon of light and then it transits into a singlet excited state. This singlet excited state dye molecule enters into a triplet state through intersystem crossing, and the excited triplet state dye molecule reacts with an electron donor. Then a proton is lost and a free radical is formed, and the dye is bleached at the same time. This free radical in the presence of the monomer initiates the polymerization reaction which continues until a termination reaction occurs.

When a photopolymer material is irradiated at the wavelength of sensitization of the dye, the related photochemical reaction occurs and the transmittance of material will also change continuously. Temporal variations of the transmittance $T(t)$ have been fitted with a photobleaching model which is developed on the basis of a previous researcher's work,[7]

$$T(t) = \frac{T_{\rm sf}}{1 + (\mathrm{e}^{\varepsilon d[D]_0} - 1)\mathrm{e}^{-\varepsilon\phi I_0 t}}, \tag{1}$$

where $T_{\rm sf}$ is a parameter related to the scattering loss of materials, d is the thickness of the photopolymer film, $[D]_0$ is the initial concentration of dye in the film, ε is the molar absorption coefficient, ϕ is the quantum yield for the generation of radicals and I_0 is the exposure intensity. Applying the non-linear fitting based on Levenberg–Marquardt's algorithm to the transmittance experimental curves, values of the molar absorption ε, the quantum yield ϕ and the intensity loss coefficient $T_{\rm sf}$ can be obtained. Simultaneously, the photobleaching coefficient $k_{\rm p}$ is obtained from the following formula: $k_{\rm p} = \varepsilon\phi I_0$.[8]

2.2. Polymerization-driven diffusion model

The intensity distribution of a sinusoidal interference pattern from coherent beams with the same intensities can be expressed as

$$I(x) = I_0[1 + \cos(K_{\rm g}x)], \tag{2}$$

where $K_{\rm g}$ is the grating wave number, and I_0 is the average recording intensity. Because the conversion of monomer into polymer is more rapid in the bright regions than in the dark ones, we assume that the free monomer concentration $\phi^{(\rm m)}(x,t)$ and polymer concentration $\phi^{(\rm p)}(x,t)$ present a sinusoidal trend, the former has a phase shift of 180° with respect to the intensity pattern, and the latter is in phase congruency with it.

$$\phi^{(\rm m)}(x,t) = \phi_0^{(\rm m)}(t) - \phi_1^{(\rm m)}(t)\cos(K_{\rm g}x), \tag{3}$$

$$\phi^{(\rm p)}(x,t) = \phi_0^{(\rm p)}(t) + \phi_1^{(\rm p)}(t)\cos(K_{\rm g}x). \tag{4}$$

As a result of polymerization, the concentration of monomer decreases with time. Simultaneously, with the gradient of monomer concentration established between the unexposed and exposed zones, the free monomer diffuses continuously from the dark to the bright regions. So variations of the monomer and polymer concentrations, with these two processes taken into account, can be expressed as

$$\frac{\partial\phi^{(\rm m)}}{\partial t} = -k_{\rm R}(t)I^{\delta}(x)\phi^{(\rm m)}(x,t) + \frac{\partial}{\partial x}D\frac{\partial}{\partial x}\phi^{(\rm m)}(x,t), \tag{5}$$

$$\frac{\partial \phi^{(\mathrm{p})}}{\partial t} = k_{\mathrm{R}}(t) I^{\delta}(x) \phi^{(\mathrm{m})}(x,t), \tag{6}$$

where D is the diffusion constant related to temperature and the physical property of materials, $k_{\mathrm{R}}(t)$ is the polymerization rate, and δ is the reaction rate constant. The value of δ is taken to be 1, i.e. $\delta = 1$, because this photopolymerization is a first order reaction.

Substituting expressions (2)–(4) into Eqs. (5) and (6) respectively, we arrive at the following first-harmonic equations of the monomer and the polymer concentrations, which can be derived:

$$\frac{\mathrm{d}\phi_0^{(\mathrm{m})}}{\mathrm{d}t} = -k_{\mathrm{R}}(t) I_0 \left(\phi_0^{(\mathrm{m})} - \frac{1}{2}\phi_1^{(\mathrm{m})} \right), \tag{7}$$

$$\frac{\mathrm{d}\phi_1^{(\mathrm{m})}}{\mathrm{d}t} = k_{\mathrm{R}}(t) I_0 (\phi_0^{(\mathrm{m})} - \phi_1^{(\mathrm{m})}) - \frac{\phi_1^{(\mathrm{m})}}{\tau_{\mathrm{D}}}, \tag{8}$$

$$\frac{\mathrm{d}\phi_0^{(\mathrm{p})}}{\mathrm{d}t} = k_{\mathrm{R}}(t) I_0 \left(\phi_0^{(\mathrm{m})} - \frac{1}{2}\phi_1^{(\mathrm{m})} \right), \tag{9}$$

$$\frac{\mathrm{d}\phi_1^{(\mathrm{p})}}{\mathrm{d}t} = k_{\mathrm{R}}(t) I_0 (\phi_0^{(\mathrm{m})} - \phi_1^{(\mathrm{m})}). \tag{10}$$

The form for the Fourier components of the spatial distribution of the refractive index in the photopolymer medium can be expressed as[13]

$$n(x,t) = n_0 + n_1(t)\cos(K_{\mathrm{g}} x) + n_2(t)\cos(2K_{\mathrm{g}} x) + \ldots . \tag{11}$$

Only by retaining the first two terms can expression (11) be converted into

$$n(x,t) = n_0 + n_1(t)\cos(K_{\mathrm{g}} x), \tag{12}$$

where n_0 is the initial refractive index of the material, and $n_1(t)$ is the refractive index modulation. Generally, taking into account the difference in refractive index among polymer, monomer and binder, the first-harmonic equation of the refractive index modulation of the material can be used as[14]

$$n_1 = C_1[-C_2\phi_1^{(\mathrm{m})} + C_3\phi_1^{(\mathrm{p})}], \tag{13}$$

where

$$C_1 = \frac{(n_0^2+2)^2}{3n_0},$$

$$C_2 = \left(\frac{n_{\mathrm{m}}^2 - 1}{n_{\mathrm{m}}^2 + 2} - \frac{n_{\mathrm{b}}^2 - 1}{n_{\mathrm{b}}^2 + 2} \right),$$

and

$$C_3 = \left(\frac{n_{\mathrm{p}}^2 - 1}{n_{\mathrm{p}}^2 + 2} - \frac{n_{\mathrm{b}}^2 - 1}{n_{\mathrm{b}}^2 + 2} \right),$$

n_{m}, n_{p} and n_{b} are the refractive indices of the monomer, polymer and binder respectively.

It is assumed that there is only monomer evenly distributed in the material with concentration ϕ_0 representing the volume fraction before exposure, so

$$\phi_1^{(\mathrm{m})}(0) = \phi_0^{(\mathrm{p})}(0) = \phi_1^{(\mathrm{p})}(0) = 0, \text{ and } \phi_0^{(\mathrm{m})}(0) = \phi_0.$$

It is provided that the polymerization rate is constant, $k_{\mathrm{R}}(t) = k_0$, so the expression (13) becomes

$$n_1(t) = \frac{2C_1\phi_0}{2 + I_0 k_0 \tau_{\mathrm{D}}} \left(\begin{array}{l} \dfrac{1}{\sqrt{1 + 2I_0^2 k_0^2 \tau_{\mathrm{D}}^2}} \exp\left[-\left(I_0 k_0 + \dfrac{1}{2\tau_{\mathrm{D}}} \right) t \right] \\ \times \left\{ \begin{array}{l} \left[(C_3 - C_2)\, I_0^2 k_0^2 \tau_{\mathrm{D}}^2 - C_3 \right] \times \sinh\left(\dfrac{\sqrt{1 + 2I_0^2 k_0^2 \tau_{\mathrm{D}}^2}}{2\tau_{\mathrm{D}}} t \right) \\ -C_3 \sqrt{1 + 2I_0^2 k_0^2 \tau_{\mathrm{D}}^2} \cosh\left(\dfrac{\sqrt{1 + 2I_0^2 k_0^2 \tau_{\mathrm{D}}^2}}{2\tau_{\mathrm{D}}} t \right) \end{array} \right\} + C_3 \end{array} \right), \tag{14}$$

where τ_{D} is the diffusion time constant which is defined as $\tau_{\mathrm{D}} = 1/DK_{\mathrm{g}}^2$. The maximum value of $n_1(t)$ is the maximal refractive index modulation Δn, which can be expressed by finding the derivative of the function (14) as

$$\Delta n = \frac{2C_1 C_3 \phi_0}{2 + I_0 k_0 \tau_{\mathrm{D}}}. \tag{15}$$

So k_0 and τ_{D} are important parameters characterizing the dynamic process of the holographic grating formation, and they are also decisive factors influencing the refractive index modulation. According to Kogelnik's coupled wave theory, the diffraction efficiency for an unslanted lossy grating without absorption can be expressed as[18]

$$\eta = D_{\mathrm{sf}} \sin^2\left(\frac{n_1(t)\pi d}{\lambda \cos\theta} \right), \tag{16}$$

where $D_{\rm sf}$ is the coefficient related to scattering loss of the gratings. Exposure sensitivity is another important parameter of the photopolymer medium, and it is a direct factor affecting the recording rate and intensity loss, and it is normally defined as $S = \sqrt{\eta_{\max}}/E$.

Quantitative information of the different parameters is obtained by fitting experimental data of the temporal evolution of the diffraction efficiency to the theoretical model based on Levenberg–Marquardt's algorithm,[19] such as that of the intensity loss coefficient $D_{\rm sf}$, the polymerization rate k_0 and the diffusion time constant $\tau_{\rm D}$.[20]

3. Experiment

3.1. Sample preparation

Under 40%–60% relative humidity and 20 °C–25 °C temperature, the photopolymerizable solution is prepared by adding a proportionally mixed dye solution together with a solution which contains 0.34 mol/L AA, 0.054 mol/L N, N'-methylenebisacrylamide (BAA) and 0.27 mol/L triethanolamine (TEA) to a 10 wt% PVA solution. The dye solution consists of Riboflavin (RF), Erythrosin B (ErB) and Methylene blue (MB) with the same densities. Pour an appropriate amount of the resulting solution onto a well-cleaned glass substrate and dry it for 24–48 h in a dark room. A photopolymer film with a thickness of about 300 μm is obtained.

3.2. Experimental setup

The experimental setup is shown in Fig. 2. An argon laser with wavelengths of 514 nm, 488 nm, and 476 nm and a He–Ne laser at 633 nm is respectively used to produce diffraction gratings by means of continuous laser exposure. BS is the beam splitter, and the laser beam is split into two secondary beams with an intensity ratio of 1:1. M_1, M_2, M_3, and M_4 are mirrors. SH_1, SH_2, SH_3, and SH_4 are shutters. SF_1 and SF_2 are spatial filters. L_1 and L_2 are Fourier lenses with focal length f, for setting up a $4f$ system. PM is the laser power meter, which is monitored in real time with a computer. We shut off SH_3 when we test the transmittance of the sample film, and make sure that the film is irradiated perpendicularly. When we test the diffraction efficiency of the gratings, we make sure that the two incident beams are recombined in the sample film at an angle 45° with respect to the normal of film and the reconstruction beam is positioned at Bragg's angle.

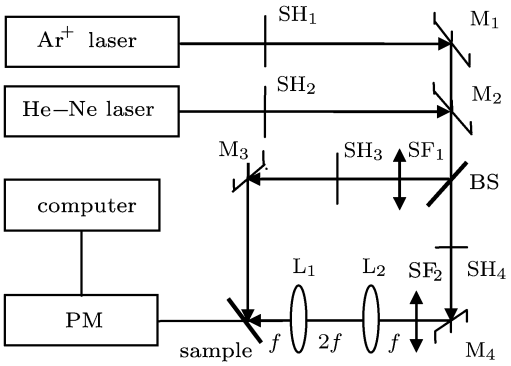


Fig. 2. Experimental setup.

4. Results and discussion

4.1. Absorption spectral characteristics

The absorption spectrum of photopolymer film is measured with a UV–visible–near infrared spectrophotometer (US, Varian Ltd., Cary5000), which is shown in Fig. 3. The absorption spectrum ranges from 300 nm to 700 nm and covers all bands of visible light, and the absorbency of materials is rugged at different wavelengths and includes three absorption peaks which are respectively nearby 664 nm, 525 nm and 457 nm. It illuminates that the sensitivity of the sample to wavelength is different in the photopolymer. So the exposure wavelength has an important effect on photochemical characteristics of materials. These absorption peaks are independent of each other, so the photopolymer film is suitable for irradiation by many conventional lasers with several wavelengths, such as Ar^+ laser and He–Ne laser.

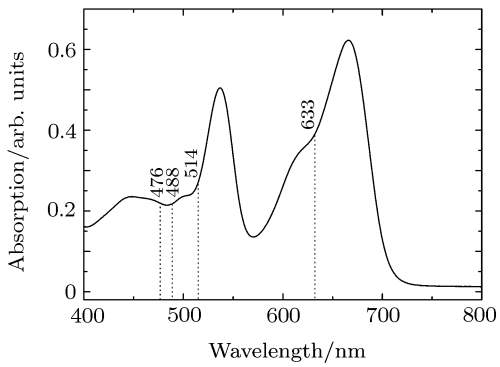


Fig. 3. Absorption spectrum of sample.

4.2. Kinetic characteristics under single wavelength laser

4.2.1. Transmittance and diffraction efficiency

According to the absorption characteristic of the photopolymer, an argon laser at a wavelength of 514 nm is used in the experiment by means of continuous laser exposure. It is convenient to obtain the transmittance and diffraction efficiency of materials for different exposure intensities. The result of fitting the transmittance curves as a function of exposure time, obtained from expression (1), is shown in Fig. 4(a). As can be seen from the figure, the theoretical fits and the experimental data are in good agreement with each other. When the exposure intensity is low, the transmittance rises slowly toward saturation as shown in Fig. 4(a) on 5.3 mW/cm^2 (curve a) and 10.6 mW/cm^2 (curve b). With exposure intensity increasing, the final transmittance also increases up to a certain value, and then it keeps constant. This behaviour can be explained by the so-called saturation effect. Laser irradiation is operated at higher intensities and the final transmittance dose not change obviously. Before saturation, the evolution of transmittance may be considered to be the breaching rate of the dye.

Figure 4(b) shows the result of the fitting of diffraction efficiency curves as a function of exposure time, obtained from expression (16). As exposure intensity increases, final diffraction efficiency increases and then decreases when the intensity is higher. The exposure intensity is low, and the diffraction efficiency is also low. As the exposure intensity increases, so does the increase rate of the diffraction efficiency. When the intensity is 21.2 mW/cm^2, the diffraction efficiency is about 53%, and then it increases slowly. When the intensity is very high, the diffraction efficiency increases rapidly in the threshold exposure time and goes to the maximum value at about 10 s, then decreases fast to 45% at 20 s. The trend of diffraction efficiency may be considered to be a characteristic of photochemistry and the diffraction of gratings. According to Kogelnik's coupled wave theory, the expression of diffraction efficiency is in the form of a sinusoidal function. In the first half period of the function, induced by increasing exposure intensity, the increase of refractive index modulation can enhance the diffraction efficiency of gratings. When the increase of exposure intensity is so big that the diffraction efficiency is beyond the first half period, it starts to decrease after the maximum value. In addition, overexposure may lead to generating a lot of radicals. They are recombined easily as a result of mutual collision among particles. This increases the rate of termination reaction, and reduces the diffraction efficiency of gratings. So the final diffraction efficiency is maximal when the intensity reaches an optimal value. From Fig. 4(b) it is implied that with the exposure intensity increasing, the maximal refractive index modulation and the exposure sensitivity also increase, but the saturation diffraction efficiency increases at first and then decreases. It illustrates that the way of blindly increasing refractive index modulation and exposure sensitivity does not mean that the diffraction efficiency can be increased.

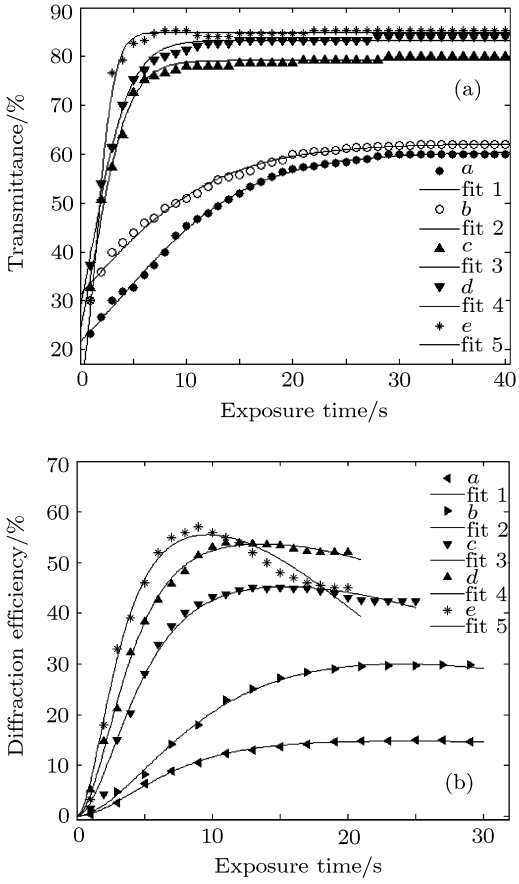


Fig. 4. Curve fittings of transmittance (a) and diffraction efficiency (b) for different exposure intensities at a wavelength of 514 nm, where the exposure intensities used are curve a 5.3 mW·cm^{-2}, curve b 10.6 mW·cm^{-2}, curve c 15.9 mW·cm^{-2}, curve d 21.2 mW·cm^{-2}, and curve e 31.8 mW·cm^{-2}.

4.2.2. Parameter fitting using experimental results

Some parameters of the theoretical model such as the molar absorption coefficient ε and quantum yield

ϕ are obtained by fitting experimental data from the temporal evolution of the transmittance, which are shown in Fig. 5. As can be seen from it, with the increase of exposure intensity, the molar absorption coefficient increases whereas the quantum yield decreases. Before the absorption of the dye reaches the saturation state, the larger the intensity is, the larger the molar absorption coefficient will be. When the intensity is low, the quantum yield is practically constant. But under strong irradiation, more triplet excited states dyes are produced. Owing to the deficient combination with the initiator, most of the triplet excited state dyes revert easily to steady state or generate dimeric species of the dye. Thus the quantum yield decreases. In addition, the parameter $T_{\rm sf}$ has no obvious change under different exposure intensities, and it is about 0.8. The values of the photobleaching coefficient $k_{\rm p}$ corresponding to five exposure conditions are respectively 0.17 $\rm s^{-1}$ (5.3 $\rm mW/cm^2$), 0.32 $\rm s^{-1}$ (10.6 $\rm mW/cm^2$), 0.42 $\rm s^{-1}$ (15.9 $\rm mW/cm^2$), 0.46 $\rm s^{-1}$ (21.2 $\rm mW/cm^2$) and 0.58 $\rm s^{-1}$ (31.8 $\rm mW/cm^2$). Because of the effect of the molar absorption coefficient, the photobleaching rate presents in increasing trend.

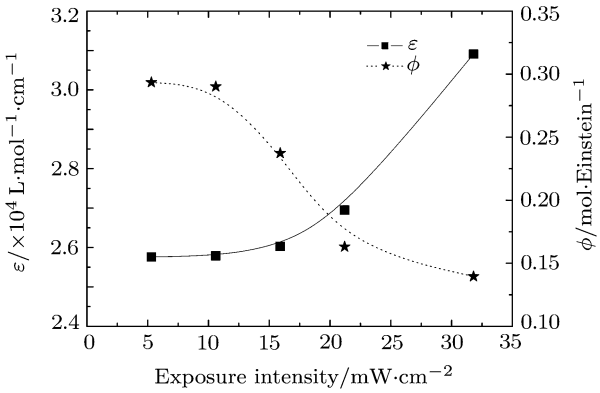


Fig. 5. Molar absorption ε and quantum yield ϕ versus exposure intensity.

Figure 6 shows parameters such as the polymerization rate k_0 and diffusion time constant $\tau_{\rm D}$ obtained by fitting experimental data of the temporal evolution of the diffraction efficiency. The polymerization rate increases as the exposure intensity rises. When the intensity is quite high, the polymerization of monomers is also very fast, thus the photopolymerization may stop earlier before monomers in the dark zone can diffuse into the bright zone. Although the diffusion time constant changes slightly, the value of $\tau_{\rm D}$ is still kept at about 100 s and it is high if compared with the typical values of diffusion times used in DuPont photopolymers. For example, with a wavelength of 514 nm the polymerization rate k_0 is 0.0049 $\rm s^{-1}$ $(\rm mW/cm^2)^{-0.74}$ and the diffusion time $\tau_{\rm D}$ is about 2 s for the DuPont HRF-150-38 photopolymer.[12] The parameter $D_{\rm sf}$, of which the value is about 0.6, has no obvious change. It is implied that an excess increase in the exposure energy results in a decrease in the diffusion time from Fig. 6.

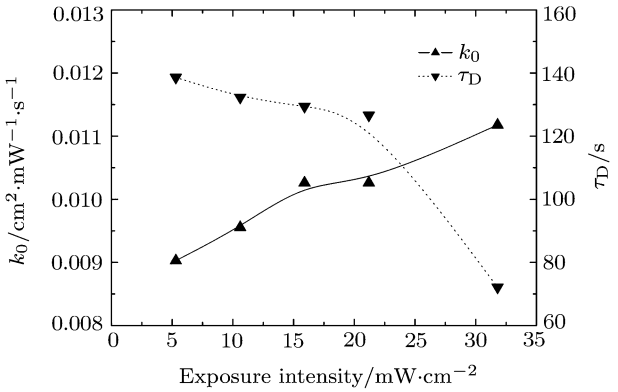


Fig. 6. Polymerization rate k_0 and diffusion time constant $\tau_{\rm D}$ versus exposure intensity.

4.3. Kinetic characteristics with multi-wavelength

4.3.1. Transmittance and diffraction efficiency

Argon lasers at wavelengths of 476 nm, 488 nm and 514 nm and a He–Ne laser at 633 nm are used in the experiment by means of continuous laser exposure, and the exposure intensity is about 10 $\rm mW/cm^2$. According to the theoretical model, we respectively fit the experimental data of transmittance and diffraction efficiency of materials at different wavelengths in Figs. 7(a) and 7(b). As can be seen from Fig. 7(a), the fitting is very good. The transmittance at these wavelengths goes to saturation at about 10 s and then goes to a steady state. It explains that the variation of transmission intensity is rapid with exposure time, and it is a nonlinear course. The transmittance rises as the selected exposure wavelength increases. It may be induced by the absorptions and scatterings of materials at different wavelengths. We can see from Fig. 3 that the absorptions of materials at the four wavelengths increase gradually, and the scattering noises are also different. According to the law of Rayleigh scattering, the shorter the wavelength is, the stronger the scattering of materials will be. So the intensity loss induced by the scattering of materials under a wavelength of 633 nm is smaller, and the value of the

relevant transmittance is biggest.

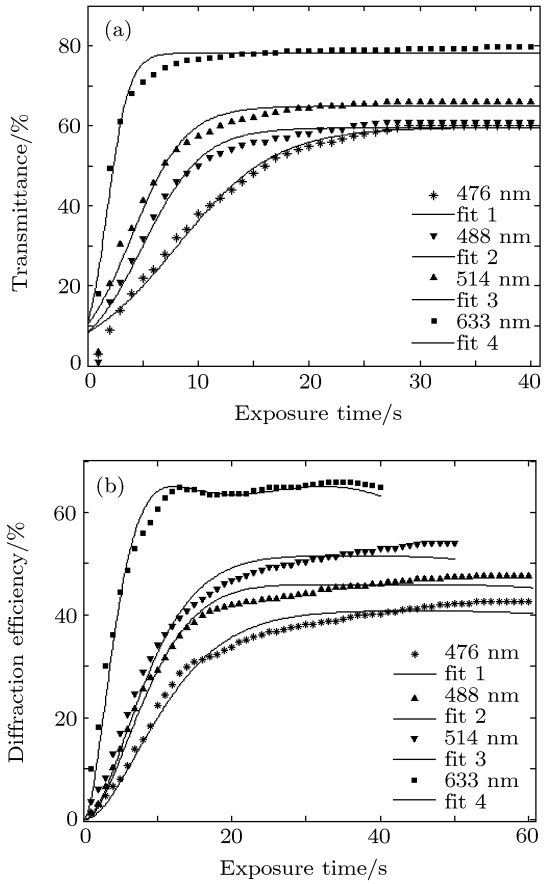


Fig. 7. Curve fittings of transmittance (a) and diffraction efficiency (b) at four wavelengths.

Figure 7(b) shows that the longer the selected exposure wavelength is, the bigger the value of diffraction efficiency will be. The reason for that may be related to the sensitivity and the scattering of materials to exposure wavelength. The trend of the diffraction efficiency curve at different wavelengths is consistent, which presents a similar phenomenon to the experimental data of diffraction efficiency of single dye sensitized photopolymer. The diffraction efficiencies at these wavelengths are above 35%, so the photopolymer material is suitable for volume holographic storage. It offers a new idea on multi-wavelength holographic storage which can extend the sensitivity range, improve the multiplicity and enlarge the storage capacity.

As can be seen from Fig. 7(b), the theoretical curve is coincident with the experimental data. The theoretical curve deviates slightly from them at longer exposure times, and it is possibly explained by the diffraction gratings gradually becoming steady due to a slight decrease of the diffusion rate induced by the decrease of concentration gradient of monomers at further exposure times.

4.3.2. Analysis of several parameters

Dynamic parameters obtained from theoretical fittings of transmittance and diffraction efficiency curves at four wavelengths are shown in Table 1. As can be seen from Table 1, the closer the exposure wavelength is to the absorption peaks of materials shown in Fig. 3, the bigger the values of ε, ϕ, $k_{\rm p}$ and k_0 will be. These results accord with the fact that the exposure sensitivity is directly correlated with the selected exposure wavelength, so using an appropriate wavelength is important to improve the storage speed of materials.

Table 1. Dynamic parameters obtained from theoretical fittings of experimental data at four wavelengths.

parameters	633 nm	514 nm	488 nm	476 nm
$\varepsilon/10^4$ L·mol^{-1}·cm^{-2}	4.03	3.60	3.55	3.52
ϕ/mol·Einstein^{-1}	0.32	0.21	0.17	0.11
$k_{\rm p}$/s^{-1}	0.58	0.34	0.28	0.17
$T_{\rm sf}$	0.78	0.74	0.69	0.68
k_0/cm^2·mW^{-1}·s^{-1}	0.044	0.026	0.024	0.021
$\tau_{\rm D}$/s	41	78.4	84.24	100.3
$D_{\rm sf}$	0.65	0.62	0.56	0.51
$S/10^{-3}$ cm^2·mJ^{-1}	2.55	1.04	0.51	0.44

5. Conclusions

A dynamic theoretical model of holographic gratings in a multi-wavelength visible light sensitive photopolymer is studied. Experimental data of transmittance and diffraction efficiency of the fabricated photopolymer at different exposure intensities and wavelengths are obtained. By fitting the data to the theoretical model,

several dynamic parameters such as the molar absorption coefficient ε, the quantum yield ϕ, the photobleaching coefficient k, the polymerization rate k_0 and the diffusion time constant $\tau_{\rm D}$ are reduced. The research shows that with exposure intensity increasing, ε, $k_{\rm p}$ and k_0 will increase, but ϕ will become smaller. These changes are similar to those of the DuPont photopolymer. With the selected exposure wavelength increasing, ε, ϕ, $k_{\rm p}$, k_0 and S also increase, but the intensity loss becomes smaller. These results accord with the fact that the photochemical property of the material and the impact of noise gratings are closely correlated with the exposure wavelength. $\tau_{\rm D}$ has no obvious changes except that the sample is overexposed. It is possible that the diffusion reaction stops earlier due to the rapid polymerization of monomers. These parameters and their variations have been seldom reported by previous research works, and they are very important for investigating photochemical and holographic characteristics of photopolymers. It is quite valuable to understand the development process of grating information and ameliorate the storage property of holographic photopolymers for high density information storage.

References

[1] Liu Y D, Gao C Q and Gao M W 2008 *Chin. Phys.* B **17** 1769

[2] Zheng Z G, Song J, Zhang L L, Liu Y G, Guo F Z, Ma J, Li W C, Deng S P and Xuan L 2008 *Chin. Phys.* B **17** 3227

[3] Gong Q X, Huang M J and Gan F X 2006 *Dyes and Pigments* **69** 204

[4] Jallapuram R, Naydenova I, Martin S, Howard R, Toal V, Frohmann S, Orlic S and Eichler H J 2006 *Opt. Mater.* **28** 1329

[5] Toishi M, Tanaka T, Watanabe K and Betsuyaku K 2007 *Jpn. J. Appl. Phys.* **46** 3438

[6] Oster G and Yang N 1968 *Chem. Rev.* **68** 125

[7] Carretero L, Blaya S, Mallavia R, Madrigal R F, Beléndez A and Fimia A 1998 *Appl. Opt.* **37** 4496

[8] Carretero L, Blaya S, Mallavia R, Madrigal R F and Fimia A 1998 *J. Mod. Opt.* **45** 2345

[9] Babeva T, Naydenova I, Martin S and Toal V 2008 *Opt. Express* **16** 8487

[10] Jallapuram R, Naydenova I, Byrne H J, Martin S, Howard R and Toal V 2008 *Appl. Opt.* **47** 206

[11] Kwon J H, Hwang H C and Woo K C 1999 *J. Opt. Soc. Am.* B **16** 1651

[12] Piazolla S and Jenkins B J 2000 *J. Opt. Soc. Am.* B **17** 1147

[13] Zhao G and Mouroulis P 1994 *J. Mod. Opt.* **41** 1929

[14] Aubrecht I, Miler M and Koudela I 1998 *J. Mod. Opt.* **45** 1465

[15] Mok F H, Tackitt M C and Stoll H M 1991 *Opt. Lett.* **16** 605

[16] Rakuljic G A, Leyva V and Yariv A 1992 *Opt. Lett.* **17** 1471

[17] Chang C C, Russell K L and Hu G W 2001 *Appl. Phys.* B **72** 307

[18] Kogelnik H 1969 *Bell Syst. Tech. J.* **48** 2909

[19] Marquardt D 1963 *SIAM J. Appl. Math.* **11** 431

[20] Neipp C, Gallego S and Ortuno M 2003 *J. Opt. Soc. Am.* B **20** 2052